ACTIVE CONTROL OF BUCKLING OF FLEXIBLE BEAMS

A. BAZ and L. TAMPE

THE CATHOLIC UNIVERSITY OF AMERICA
MECHANICAL ENGINEERING DEPARTMENT
WASHINGTON, DC 20064

A B S T R A C T

This paper investigates the feasibility of using the rapidly growing technology of the SHAPE MEMORY ALLOY actuators in actively controlling the buckling of large flexible structures.

The need for such buckling control systems is becoming inevitable as the new design trends of large space structures have resulted in the use of structural members that are long, slender and very flexible. In addition , as these truss members are subjected mainly to longitudinal loading they become susecptible to structural instabilities due to buckling. Proper control of such instabilities is essential to the effective performance of the structures as stable platforms for communication and observation.

The paper presents mathematical models that simulate the dynamic characteristics of the shape memory actuator, the compressive structural members and the associated active control system.

A closed-loop computer-controlled system is designed, based on the developed mathematical models, and implemented to control the buckling of simple beams. The performance of the computer-controlled system is evaluated experimentally and compared with the theoretical predictions to validate the developed models.

The obtained results emphasize the importance of buckling control and suggest the potential of the Shape Memory Actuators as attractive means for controlling structural deformation in a simple and reliable way.

ACKNOWLEDGEMENTS

This study was sponsored by NASA - Goddard Space Flight Center in Greenbelt, MD under grants number NAG 5-520 and NAG 5-749. Special thanks are due to Dr. Joseph Fedor , code 712, and Mr. Eric Osborne , code 716, for their invaluable technical inputs. Thanks are also due to Mr. Phil Studer , code 716, for initiating this study when he was working in NASA.

INTRODUCTION

The construction and operation of large structures , which are extremely flexible and inherently low in natural damping, have posed challenging problems particularly when these structures are used as stable platforms for communication and observation. The strict constraints imposed on the structural deflections, under loads, has necessitated the use of various types of active [1-2] and passive [3-4] control systems. Common among all these systems is the emphasis on controlling the transverse bending [5-6] and/or torsional [7] modes of the structures in one way or another. No effort has been exerted to control structural deflections resulting from axial loading. This is inspite of the fact that all the structural members, with pinned joints, are subjected primarily to axial loading. Also, as the new design trends have resulted in structural members that are long , slender and flexible , then these members become highly suscptible to structural instabilities due to buckling.

Therefore, it is the purpose of this study to investigate, both theoretically and experimentally, the feasibility of devising an active buckling control system as means for enhancing the elastic stability characteristics of compressive structural members. The study aims also at demonstrating the feasibility of using the Shape Memory Actuators, which are made of Nickel-Titanium alloy (NITINOL) [8] to control the buckling of the compressive structural members.

THE SHAPE MEMORY ACTUATOR

Background

The shape memory NITINOL actuators are selected, for this study, because of their numerous attractive features that favor them over

other viable actuators such as the piezo-electric actuators [1-2]. The NITINOL actuators are capable of generating large displacements (about 1 - 3 cm) when energized by relatively low voltages (about 5 volts) [9-10]. On the contrary, piezo-electric actuators require very high voltages (in the order of 100 to 300 volts) to produce micro-displacements as indicated in many references [11-12]. Such low excitation voltages and large displacement capabilities of the NITINOL actuators were the main reasons behind their wide utilization in numerous applications. Examples include : the HITACHI robot hand [13] and other robotic devices [14], radiator valves [15], greenhouse vents [15] , liquid gas switches [15] , etc. In all these applications NITINOL actuators have demonstrated their light weight , large force and displacement capabilities as well as low power consumption. In 1987, Baz et al [10] have successfuly used the NITINOL actuators as means for controlling the flexural vibrations of cantilever beams. Accordingly, the present study is a natural extension of that work.

Operating Principle

The shape memory actuator relies in its operation on the unique behavior of the NITINOL alloy when it undergoes a martensitic phase transformation. When the actuator, shown as a helical spring in Figure (1), is cooled below its martensitic transformation temperature and deformed, it will remember its original shape and return to it if heated back past the transformation temperature. The phase transformation to austenite produces significant forces as the alloy recovers its original shape. Therefore the alloy can act as an actuator converting thermal energy to mechanical energy. With recent advances in NITINOL technology, phase transformation temperatures of

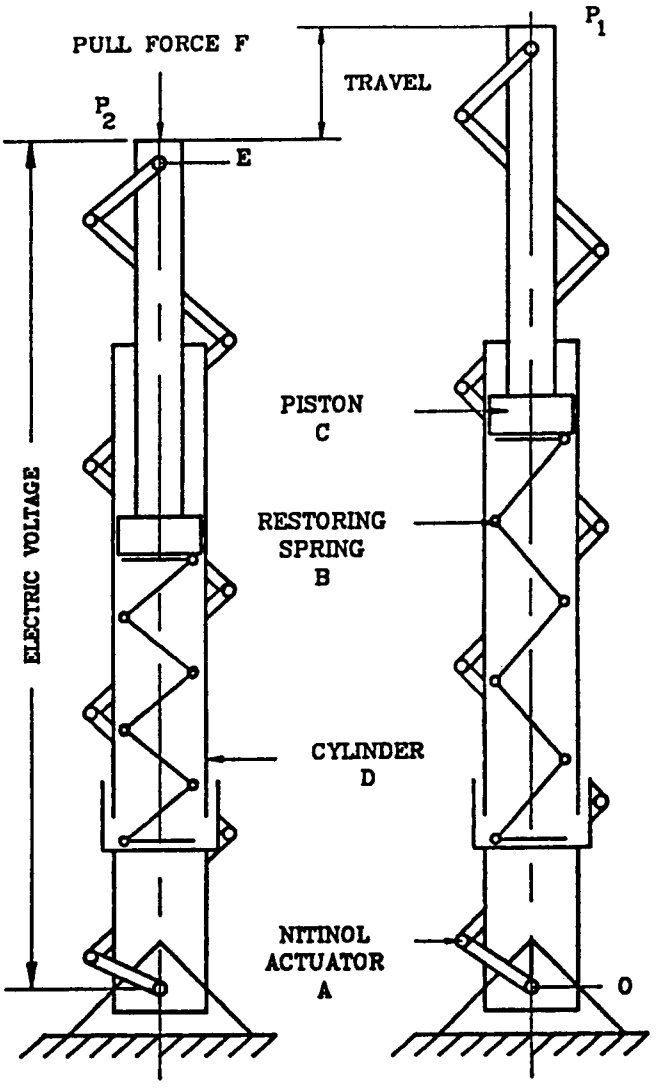

Figure (1) - A schematic drawing of a typical Shape memory NITINOL actuator.

about 40° to 50°C are common. Therefore, natural cooling of the actuator A to ambient room temperature will make it assume its martensite phase. A passive restoring spring B can be used to stretch the cold matensite actuator to assume position P_1. When heat is applied to the actuator, by passing electric current through it, it undergoes the phase transformation. The actuator shrinks to assume a memorized position P_2 and provides in the process a significant force F. This force can pull the piston C ,inside the cylinder D , moving the end E of the actuator relative to the end O.Therefore, if the two ends E and O are connected to two points on a flexible structure , the spacing between these two points can be controlled in the presence of external disturbances.

Such position memorization characteristics of the NITINOL actuator is utilized to memorize the shape of the unbuckled beam . Any deviations from this shape causes the control system to energize the actuator to bring the beam back to its memorized position.

The energy and the momentum equations that describe the thermal and dynamic characteristics of the NITINOL actuator are summarized in the appendix . For a more comprehensive analysis, the work of Baz et al [10] should be consulted . The presented equations are applied to the NITINOL actuator number 925100-01 produced by RAYCHEM corporation [16] which is used in the buckling control system developed in this study.

THE BUCKLING CONTOL SYSTEM

Figure (2) shows a schematic drawing of the system used to control the buckling of a flexible elastic member A. The member is subjected to compressive loading using a pneumatic power cylinder D which is coupled directly to the member via a movable base C. The deflection of the mid-span of the beam, during the occurrence of the buckling, is sensed by a non-contacting proximity sensor F.The sensor serves also as a physical stop to prevent the beam from undergoing excessive deflections as it buckles under load. The position signal is fed into an analog-to-digital (A/D) converter to a micro-processor to manipulate it using an ON-OFF controller with an adjustable dead-band . The computed control action is sent via a digital-to-analog (D/A) converter to a power amplifier to provide the power necessary to drive the NITINOL actuator G . When energized , the actuator shrinks pulling the power piston upward to reduce its lateral deflection and prevent the occurrence of buckling.

When the actuator brings the beam back to its unbuckled position , the computer de-energizes the actuator by turning off its power. The actuator cools down , past its martensitic transformation temperature, and returns back to its original position under the action of the restoring spring H.

Figure (3) shows a block diagram of the devised control system.

The evaluation of the control system performance is achieved by monitoring the pressure of the compressed gas powering the pneumatic cylinder , which is proportional to the applied compressive load, using a pressure transducer E. The transducer output signal is plotted as a function of time on a chart recorder along with the corresponding

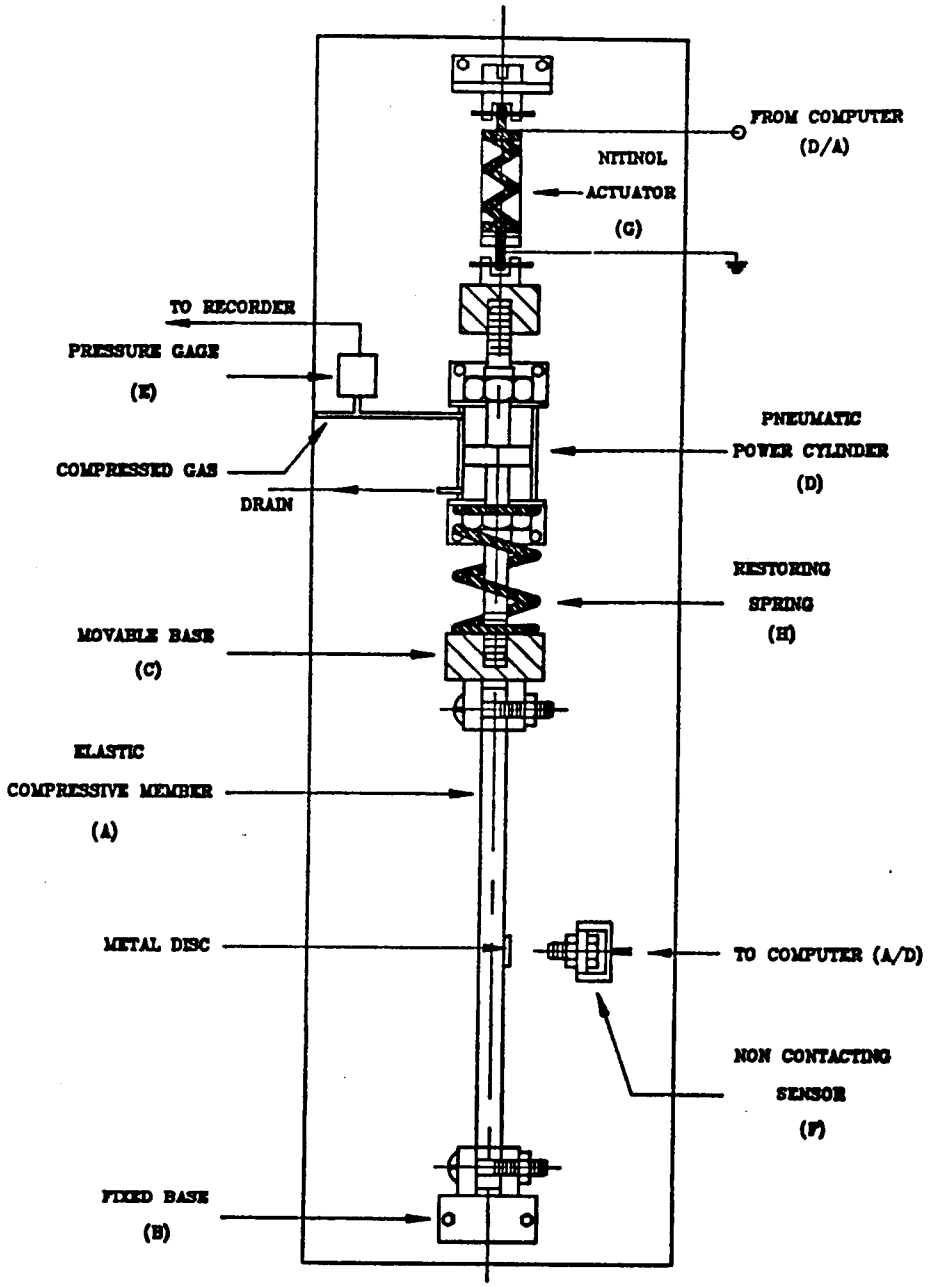

Figure (2) - A schematic drawing of the buckling control system.

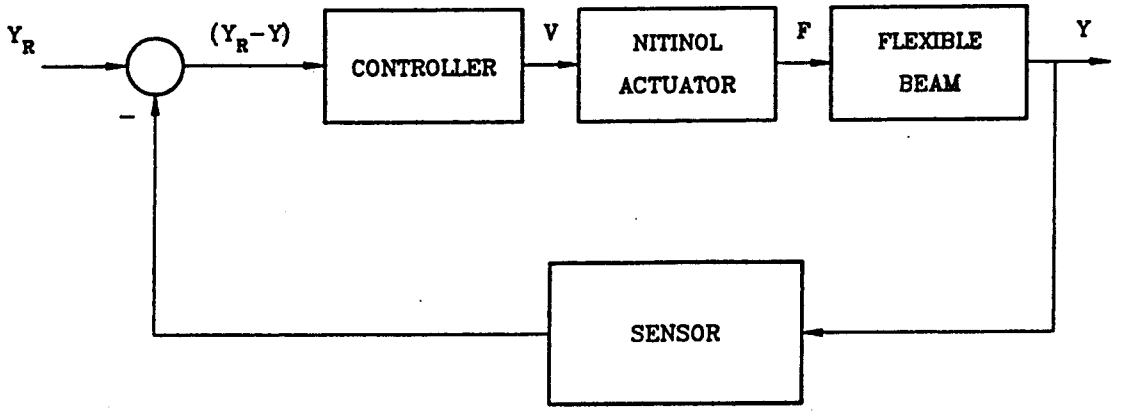

Figure (3) - A block diagram of the buckling control system.

beam position signal.

MODELING OF THE BEAM DYNAMICS

The dynamic characteristics of the flexible beam under the action of external compressive loading and the action of the NITINOL actuator are determined by considering the finite element model of the compressive member shown in Figure (4). The model presented is based on the linear theory of small deflections.

Stiffness matrix of the beam element

The element stiffness is determined by equating the strain energy, resulting from the deflection of each element, to the work done by the external forces gives

$$E\,I \int_0^{l} (d^2y/dx^2)^2\,dx = \delta^T q + P \int_0^{l} (dy/dx)^2\,dx \qquad (1)$$

where **EI** is the flexural rigidity of the element, l is the element length, δ is the deflection vector of the nodal points bounding the element and **y** is the transverse deflection of any point along the **x** axis of the beam.

The LHS of equation (1) is the strain energy whereas the first term of the RHS is the work done by the transverse loads **q** and the second term is the work done by the resultant compressive loads **P**.

Defining the element stiffness K_i by

$$q = K_i \delta \qquad (2)$$

Then equation (1) can be used, along with a properly selected deflection function [19], to give the element stiffness matrix K_i as

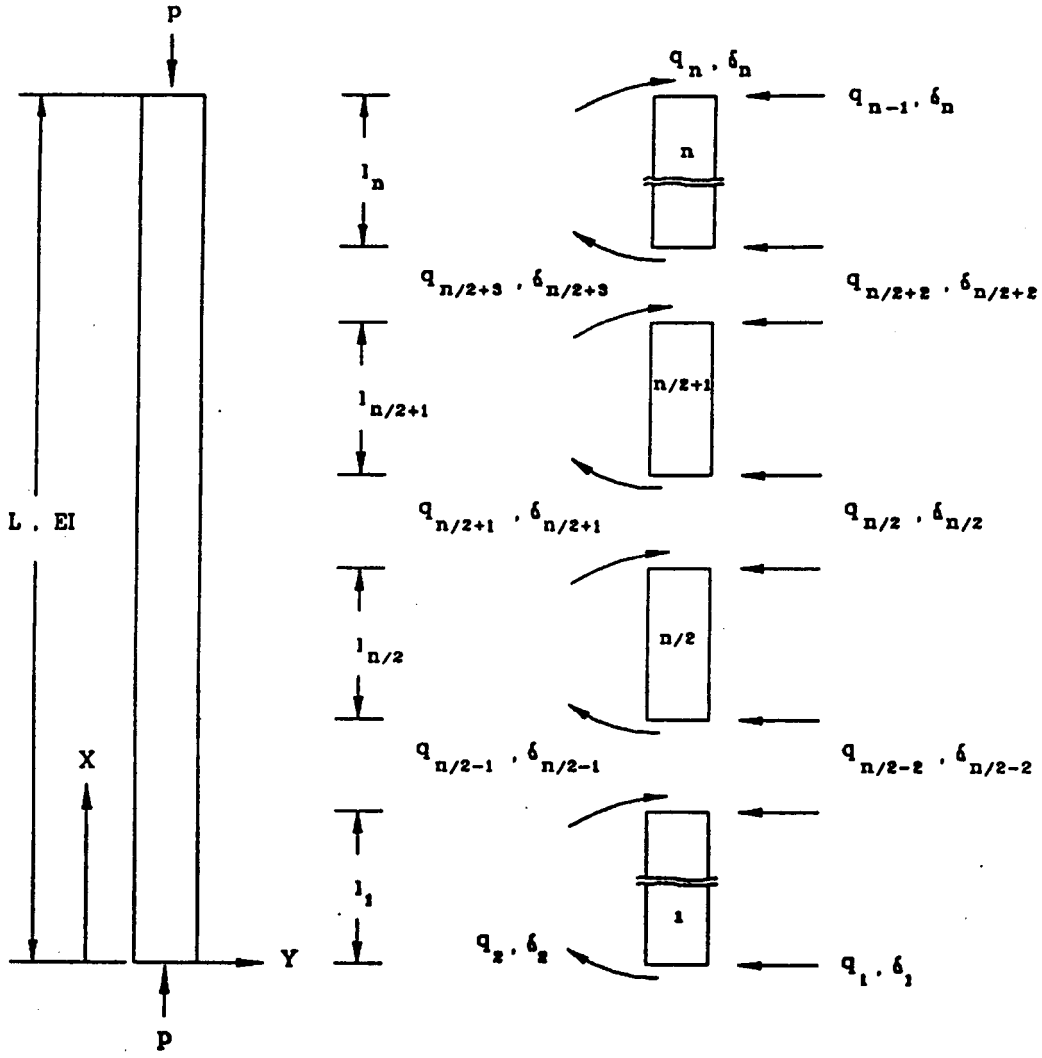

Figure (4) - The finite element of a beam subjected to axial and transverse loadings.

follows :

$$K_i = \frac{EI}{l^3}\begin{bmatrix} 12 & -6l & -12 & -6l \\ -6l & 4l^2 & 6l & 2l^2 \\ -12 & 6l & 12 & 6l \\ -6l & 2l^2 & 6l & 4l^2 \end{bmatrix} - \frac{P}{30l}\begin{bmatrix} 30 & -3l & -36 & -3l \\ -3l & 4l^2 & 3l & -l^2 \\ -36 & 3l & 36 & 3l \\ -3l & -l^2 & 3l & 4l^2 \end{bmatrix} \quad (3)$$

It can be seen that the element stiffness matrix consists of two matrices : the first is the conventional transverse stiffness and the second represents the reduction effect that the compressive axial loading has on the bending stiffness. Accordingly, as the axial load is increased the bending stiffness decreases and eventually vanishes as the axial load becomes equal to the critical buckling load.

The overall stiffness matrix **K** of the beam can then be determined by combining the stiffness matrices of the individual finite elements making up the beam . The principle of superposition is used in this regard as shown , for example, in Ref.[19] and [20].

Mass matrix of the beam

The inertial properties of the beam are determined by assuming the mass and the inertia of the beam to be lumped at the nodal points [20] . This gives the mass matrix **M** as follows :

$$M = \begin{bmatrix} m_1 & & & & \\ & J_1 & & & \\ & & .. & & \\ & & & m_n & \\ & & & & J_n \end{bmatrix} \quad (4)$$

where m_i and J_i are the equivelant mass and mass moment of inertia of the beam elements connected to node i.

Equation of motion of the beam

The overall stiffness and mass matrices (K and M)are used to form the equation of motion of the beam as follows :

$$M \ddot{\delta} + K \delta = q \qquad (5)$$

where δ and $\ddot{\delta}$ are the deflection and acceleration vectors of the nodal points.

Equation (5) defines the dynamic characteristics of the flexible beam as influenced by its gemetrical , elastic and inertial parameters as well as the external transverse and axial loads (q and P). It should be pointed out that the resultant axial load P is given by:

$$P = F_p - F_a \qquad (6)$$

where F_p is the compressive axial load applied to the beam and F_a is the control force developed by the NITINOL actuator. This force is given by

$$F_a = F - F_s - F_d \qquad (7)$$

In the above equation F, F_a and F_d are the phase transformation, the spring and the damping forces of the NITINOL actuator. The phase transformation force is given by equation (A-11) in the appendix. The spring and damping forces of the actuator are determined by assuming the buckling curve to take the form :

$$y = \delta_{n/2} \sin (\pi x / L) \qquad (8)$$

where $\delta_{n/2}$ is transverse deflection of the mid-span point of the beam. Such deflection can be related ,geometrically, to the axial deflection x of the beam-actuator system as follows :

$$x = 1/2 \int_0^L (dy/dx)^2 \, dx \ , \qquad (9)$$

which yields

$$x = (\pi \delta_{n/2})^2 / (4 L) \qquad (10)$$

Accordingly,

$$F_s = K_a x = K_a (\pi \delta_{n/2})^2 / (4 L) \ , \qquad (11)$$

and

$$F_d = C_a \dot{x} = [C_a \pi^2 \delta_{n/2} / (2 L)] \dot{\delta}_{n/2} \qquad (12)$$

i.e. these two forces are related to the transverse deflection $\delta_{n/2}$ and velocity $\dot{\delta}_{n/2}$ of the mid-span point of the beam. In equations (11) and (12) , K_a and C_a are the stiffness and the damping coefficient of the actuator.

ANALYSIS OF THE BUCKLING CONTROL SYSTEM

The presented dynamic model of the flexible beam is coupled with the NITINOL actuator model , given in the appendix, to predict the performance of the buckling control system under different operating and design conditions.

Figure (5) shows the flow chart of the computational algorithm used to analyze the performance of the control system. The algorithm is applied to a fixed-fixed flexible beam whose main geometrical and physical properties are given in Table (1).

Table (1) - Geometrical and physical properties of the flexible Beam

Length (cm)	Width (cm)	Thickness (cm)	Young's Modulus (G N/m^2)	Density (gm/cm^3)
125	2.5	0.3125	2.8	1.2

For such a beam the critical buckling load , based on Euler's theory , is 4.4 N (or 1 pound) [19].

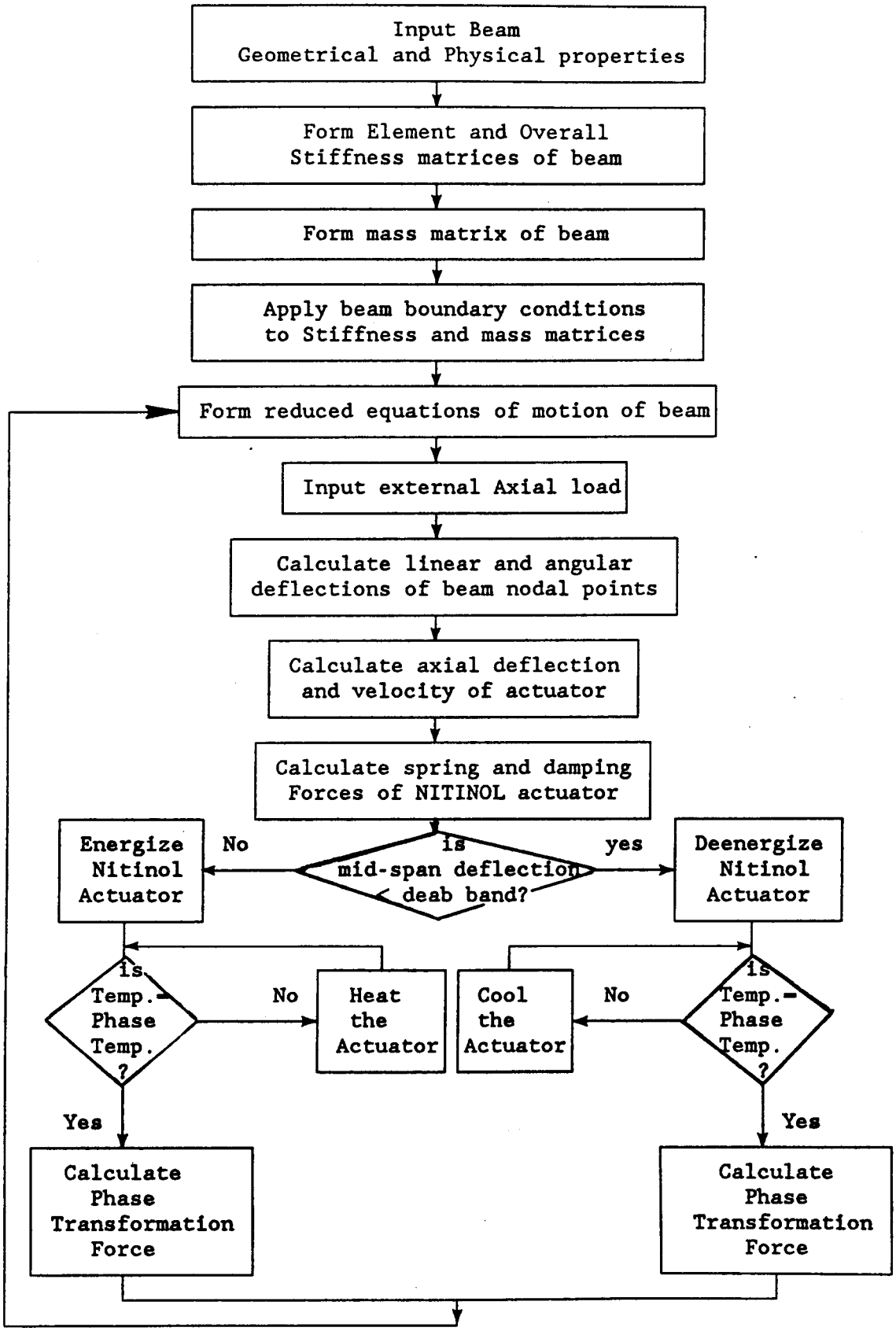

Figure (5) - Flow chart of the computational algorithm.

A typical theoretical response characteristics of the flexible beam is shown in Figure (6) when it is subjected to a gradually increasing axial force. The time history of such axial load is shown in Figure (6-a) indicating a uniform and very slow rise rate of 0.0917 N/s. It can be seen that the uncontrolled beam , which is originally displaced from the vertical by 0.125 mm (0.005 in), buckles when the axial load reaches the critical load. . This occurs after a time of 55.9 seconds as shown in Figure (6-b). The figure shows also the time response of the beam when controlled by five NITINOL actuators with a dead band of 0.3125 mm. In this case the actuators are energized by 1.6 volts. It is evident that the beam does not buckle even when the applied axial load exceeds the critical load. The actuators control forces counterbalance the applied load and prevent the beam from buckling beyond the set dead band . Figure (6-c) displays the corresponding time history of the actuators control forces. It is clear that the actuators are energized when the beam starts to buckle after 55.9 seconds. But, once the actuators forces build to a level that brings the axial load below the critical load and the beam deflection below the set dead band then the controller de-energizes the actuators. This is manifested clearly by the exponetial drop of the actuators forces . However, as the axial load increases again beyond the critical load the controller energizes the actuators again to avoid the occurrence of buckling . Such a process repeats itself over and over again as can be seen from Figure (6-c). It is important to note that the beam remains unbuckled inspite of the continuous increase of the applied axial load . The reason for this phenomenon is attributed to the fact that the actuators forces build up continuously to match the increase in the axial load. Such an

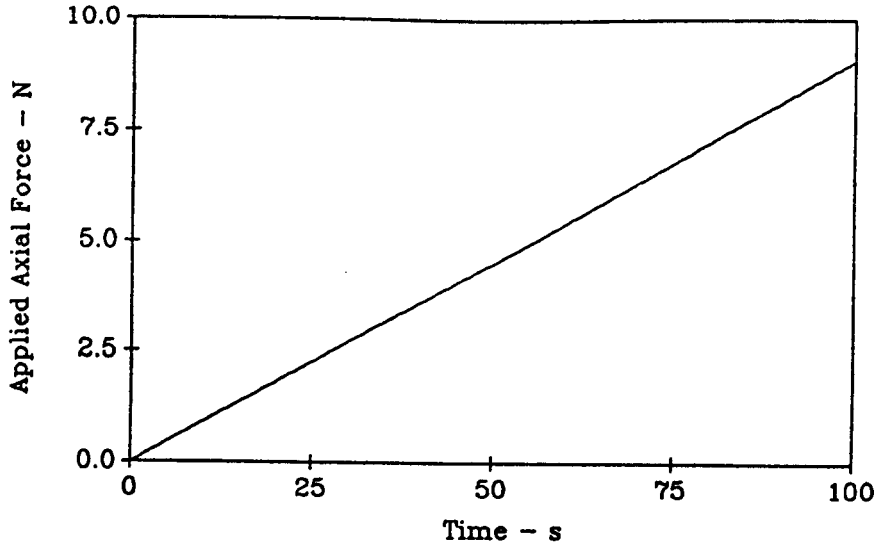

Figure (6-a) - Time history of the applied axial load.

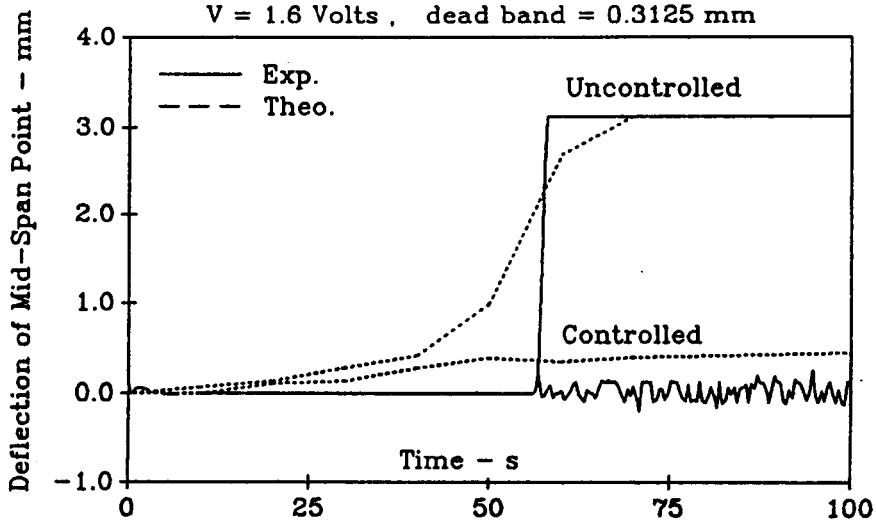

Figure (6-b) - Theoretical and experimental time response of the uncontrolled and controlled beam.

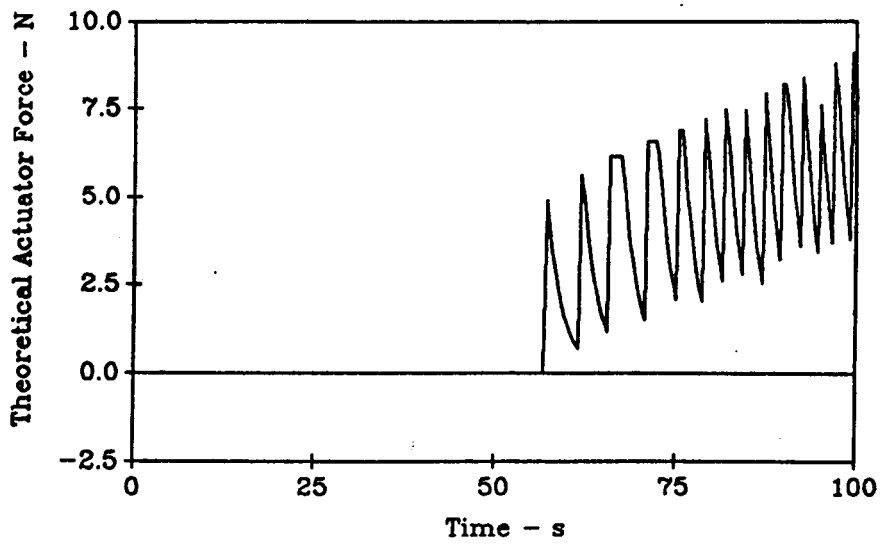

Figure (6-c) - Theoretical time history of the actuator control force.

increasing trend of the actuators forces is seen clearly from Figure (6-c). Obviously, the beam will eventually buckle when the actuators forces reach their maximum limit and become incapable of counter-acting the effect of the continuously increasing axial load.

Figure (6-b) shows also a comparison between the theoretical and experimental time responses of the uncontrolled and the controlled beam. The figure indicates that there is a close agreement between the experimental results and the theoretical predictions.

E X P E R I M E N T A L R E S U L T S

The performance of the buckling control system is measured for different widths of the controller dead band and various values of the actuators' energization voltage.

Figure (7) shows the experimental time responses of the beam when the energization voltage is 1.6 volts and for three values of the controller dead band. The presented results indicate that the performance of the controller deteriorates as the width of the dead band is increased. The controller performance degrades also when the actuators' energization voltage is reduced as can be seen from Figure (8).

C O N C L U S I O N S

This paper has presented , for the first time, a new class of active control systems to control the buckling of elastic beams. Such systems add a new dimension to the present state-of-the-art which concentrates mainly on the control of transverse or torsional

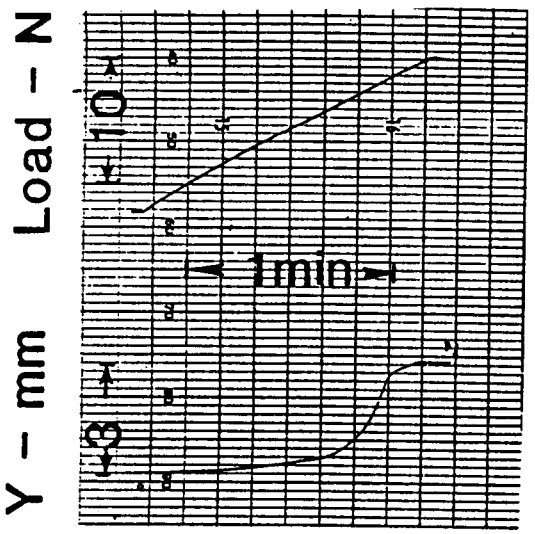

Uncontrolled

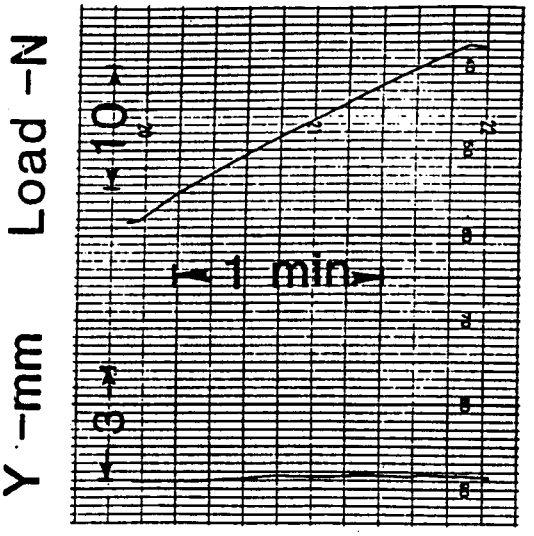

dead band 0 mm

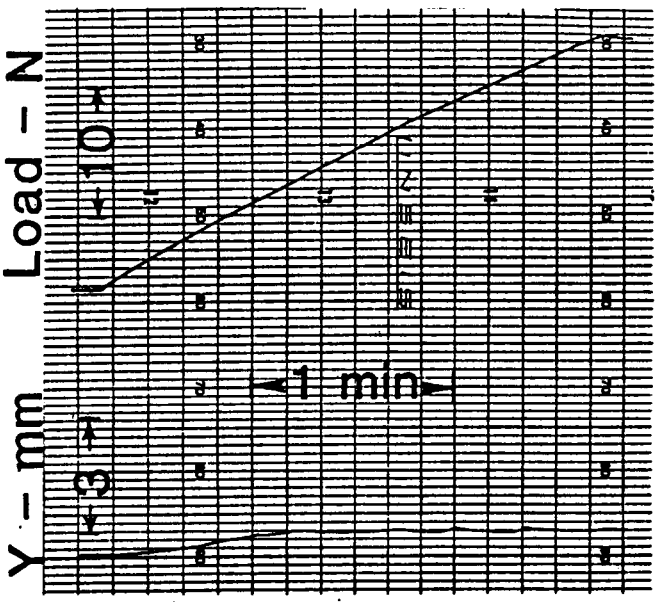

dead band .156 mm

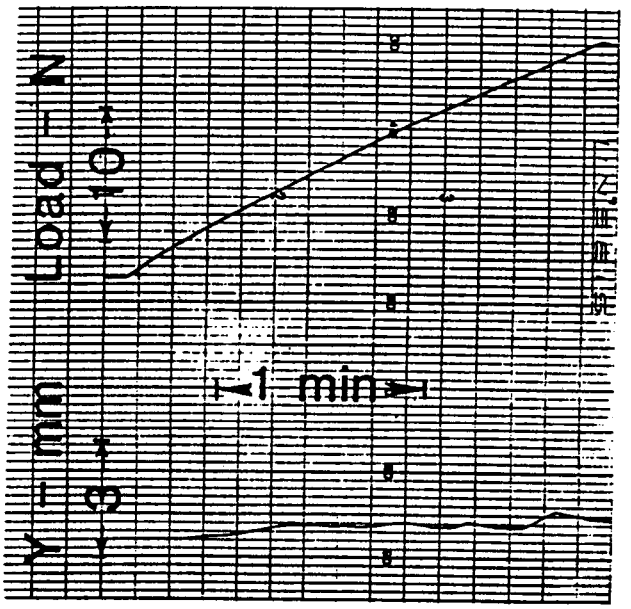

dead band .31 mm

Figure (7) - Effect of varying the width of the controller dead band on the beam time response when the energization voltage = 1.6 volts.

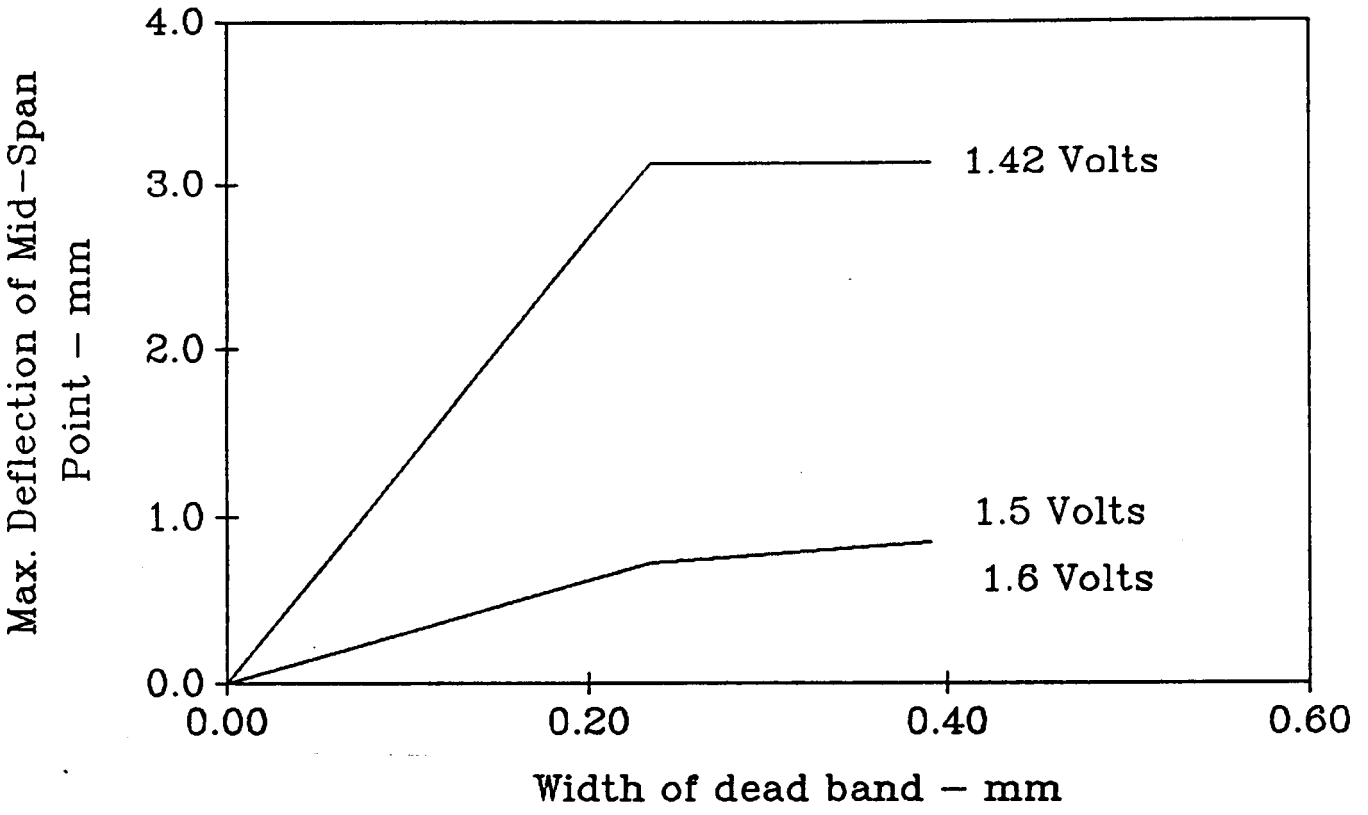

Figure (8) - Effect of dead band and actuator voltage on the maximum deflection of the beam.

vibrations of flexible structures. The devised controller relies in its operation on the use of shape memory NITINOL actuators. Theoretical models have been developed to describe the dynamics of the NITINOL actuator , the flexible beam and the control system. The validity of the developed models has been checked against experimental results. The obtained results indicate close agreement between the experimental results and the theoretical predictions. Furthermore, the testing of a computer-controlled system demonstrated the feasibility of the active control system in preventing the buckling of a flexible beam. Also, the results obtained suggest the potential of using NITINOL actuators as attractive alternative to the presently available types of actuators. The implementation of the controller is seen to be very simple and the actuators are found to require low excitation voltages to produce large control forces and deflections.

The mathematical models presented in this study provides invaluable tools for the design and the analysis of NITINOL actuators and their associated control systems.

A P P E N D I X

M A T H E M A T I C A L M O D E L I N G of T H E D Y N A M I C S of N I T I N O L A C T U A T O R S

A mathematical model is developed to describe the dynamic characteristics of NITINOL actuators. It incorporates the energy and momentum equations as well as the phase transformation relationships.

1. *The energy and phase transformation equations*

When a voltage V and a current I are applied suddenly to the NITINOL actuator , as shown in Figure (A-1-a) ,its temperature T rises from ambient temperature T_a according to the following energy equation

input energy = lost energy + stored energy

$$V I = -h A (T- T_a) + m c_p dT/dt \qquad (A-1)$$

Figure (A-1-b) shows a typical temperature history of the actuator when subjected to step input voltage. The actuator temperature T rises in an exponential form as dictated by equation (A-1). When the actuator temperature reaches the phase transformation temperature T_T , it remains constant until the phase transformation process is completed. The time t_1 needed to reach T_T can be determined from equation (A-1) ,

$$t_1 = \tau_{th} \ln \left[1/ \left(1- (T_T-T_a)/(V I/h A) \right) \right], \qquad (A-2)$$

where τ_{th} is the thermal time constant of the actuator , given by

$$\tau_{th} = m c_p / h A \qquad (A-3)$$

Also, the time $(t_2- t_1)$, needed to complete the phase transformation can be determined from :

$$t_2-t_1 = m Q_1 / V I = 4 \tau_h \qquad (A-4)$$

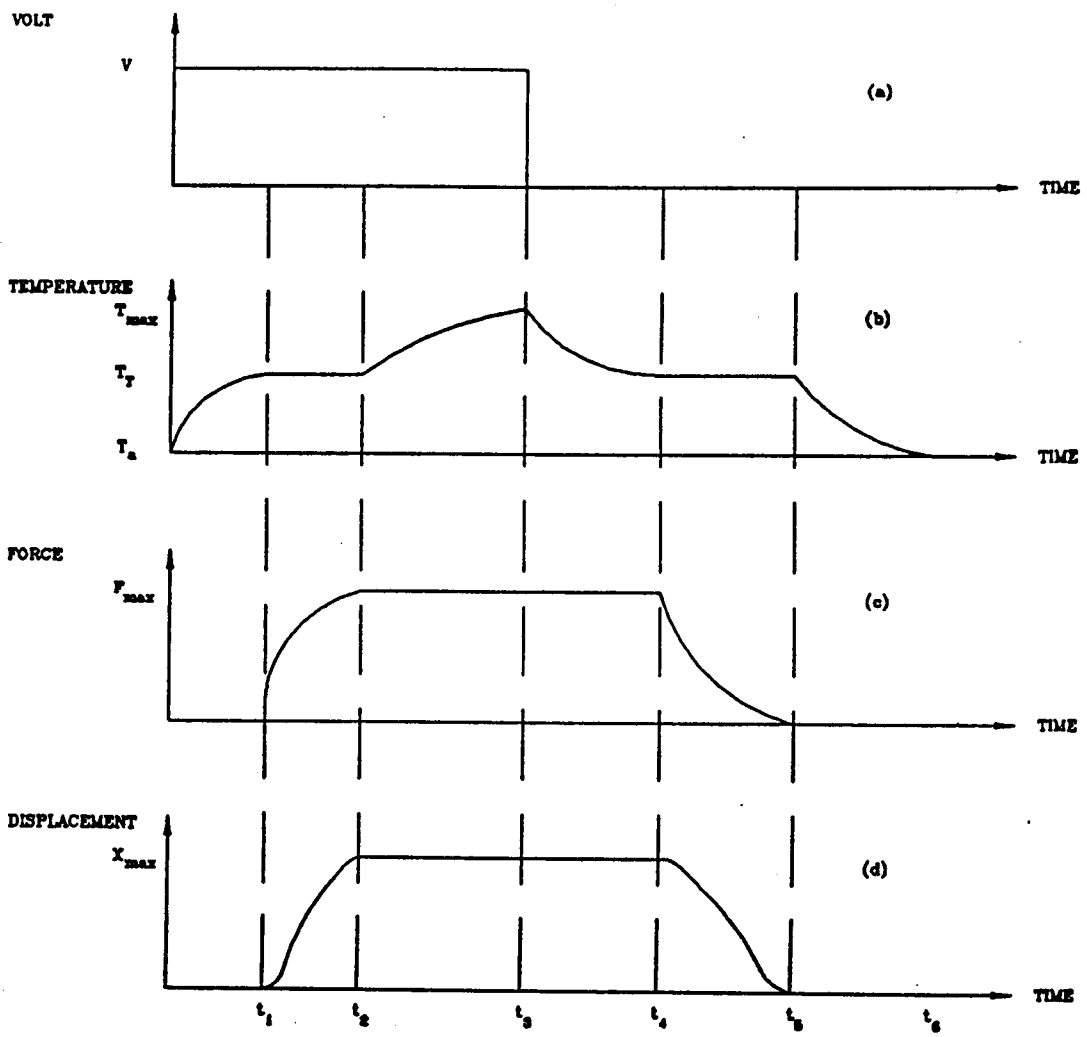

Figure (A-1) - The voltage, temperature, force and displacement profiles of a typical NITINOL actuator.

Once the phase transformation is completed , the actuator temperature starts increasing again to reach a maximum temperature T_{max} given by

$$T_{max} = T_a + V\ I\ /\ h\ A \quad , \qquad \text{(A-5)}$$

after a period $(t_3 - t_2)$, given by

$$t_3 - t_2 = \tau_{th} \ln \left[1/ \left(1 - (T_{max} - T_T)/(V\ I/hA) \right) \right] \qquad \text{(A-6)}$$

When the applied voltage is switched off suddenly, the actuator begins to cool by natural convection. After a period $(t_4 - t_3)$ given by

$$t_4 - t_3 = \tau_{th} \ln \left[(T_{max} - T_a)/ (T_T - T_a) \right] \qquad \text{(A-7)}$$

the actuator temperature reaches the martensite transformation temperature T_T. At that temperature the NITINOL starts to transform from austenite to martensite as it loses its latent heat to the ambient. This transformation occurs over a period of time $(t_5 - t_4)$ given by

$$t_5 - t_4 = m\ Q_1\ /\ [\ h\ A\ (\ T_T - T_a)\ ] = 4\ \tau_c \qquad \text{(A-8)}$$

Following the completion of this transformation process the actuator continues to cool exponentially from T_T to within 2% of T_a over a time period $(t_6 - t_5)$ given by :

$$t_6 - t_5 = \tau_{th} \ln \left[(T_T - T_a)/ 0.02\ T_a \right] \qquad \text{(A-9)}$$

Equations (A-1) through (A-9) describe completely the thermal behavior of a NITINOL actuator when subjected to step voltage changes.

2. *The momentum equation*

The motion of the NITINOL actuator is caused by the generation and the recovery of the forces resulting from its phase transformation. Figure (A-1-c) shows the history of these phase transformation forces , conforming to the temperature history outlined above. It is assumed that the forces resulting from thermal expansion

and contraction of the actuator are negligible compared to the transformation forces . Furthermore, it is assumed that the phase transformation forces are generated and recovered exponentially in time. With such assumptions, the equation of motion of the actuator can be written as :

$$m\ddot{X} + C_a\dot{X} + K_a X = F(t) \qquad \text{(A-10)}$$

where m, C_a, K_a, X and F are the equivelant mass, damping coefficient, stiffness, displacement and transformation force respectively. The transformaion force is given by :

$$\begin{aligned} F(t) &= 0 && \text{for } 0 < t < t_1 \quad [a] \qquad \text{(A-11)} \\ &= F_{max}\left[1-e^{-(t-t_1)/\tau_h}\right] && t_1 < t < t_2 \quad [b] \\ &= F_{max} && t_2 < t < t_3 \quad [c] \\ &= F_{max}\left[e^{-(t-t_4)/\tau_c}\right] && t_4 < t < t_5 \quad [d] \\ &= 0 && t_5 < t < t_6 \quad [e] \end{aligned}$$

where

$$F_{max} = K_a X_{max} \qquad \text{(A-12)}$$

with X_{max} as the maximum deflection of the actuator which is set during its training phase.

The resulting displacement of the NITINOL actuator can be obtained by integrating equation (A-10) and a typical time history will be as shown in Figure (A-1-d). It is seen that the actuator remains stationary until its temperature reaches T_I. It then starts shrinking according to the second order differential equation (A-10) under the influence of the gradually increasing transformation force F, of equation (A-12b). A final maximum deflection X_{max} is attained and maintained as long as the applied voltage remains unchanged. Once the applied voltage is switched off, the actuator will stay

stationary at X_{max} until it cools down to T_T. At this point , the phase recovery force will gradually bring the actuator back to its original position.

It is , therefore, evident that the processes of heating, phase transformation, cooling and actuator motion are interacting closely to control the operation of the actuator.

APPLICATION OF THE MODEL

The developed dynamic model of the NITINOL actuator is applied to RAYCHEM's actuator (model # 925100-01) in order to identify its basic thermal and dynamic parameters using the experimental data published by Yeager [16]. Table (A-1) summarizes the basic operating parameters of the actuator and Table (A-2) lists its main physical properties. Further measurements indicated that the actuator is made of a wire that is 0.075 cm in diameter which weighs 0.37 gm.

Using the above information, it was possible to predict the theoretical performance characteristics of the actuator. Figures (A-2-a) through (A-2-d) present comparisons between such theoretical predictions and the experimental results of Yeager [16]. Figure (A-2-a) displays the effect of the current, flowing through the actuator , on the time elapsed before the actuator starts to move and to reach 90% of its final stroke. The effects of varying the ambient temperature on the heating and cooling times are shown in Figures (A-2-b) and (A-2-c) respectively. Additional comparisons are shown in Figure (A-2-d) between the theoretical and experimental time responses of the actuator, when heated by different electric currents . In these comparisons the actuator is assumed to be critically damped with a damping coefficient of 20 Ns/m. This assumption is clearly justified

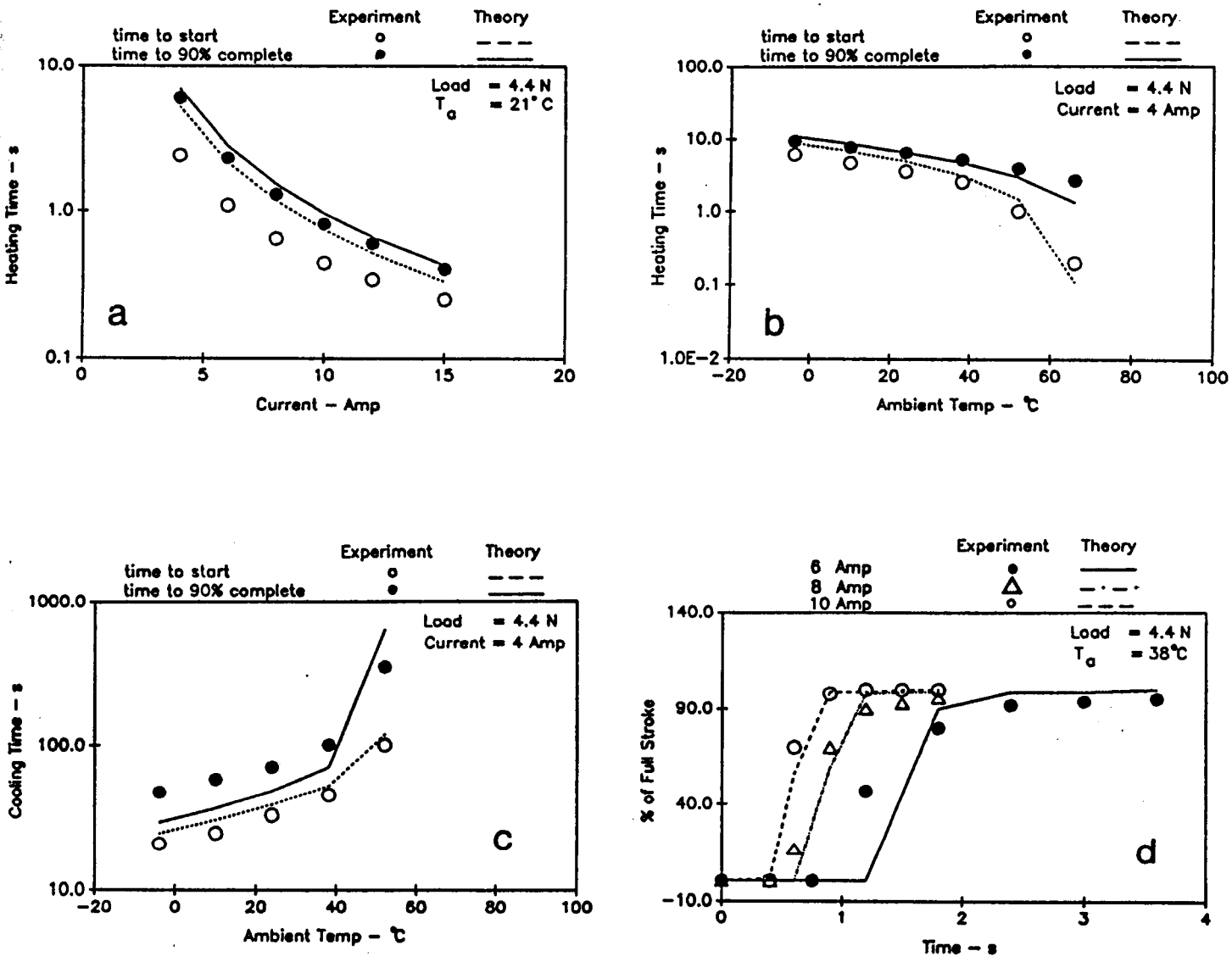

Figure (A-2) - Comparisons between theoretical and experimental characteristics of the NITINOL actuator.

by the experimental results. Also, the heat transfer coefficient h is assumed to be 18 w/m^2s^ok for natural convection in moderately still air .

With these assumptions, it is evident that the theoretical predictions are in close agreement with the measured performance charactersitics.

Table A-1 - Operating parameters of Raychem's Actuator [16]

PARAMETER	VALUE
1. stroke (X_{max})	2.5 cm
2. overall length (fully extended)	8.12 cm
3. operating force (F_{max})	4.5 N
4. overload force	6.8 N
5. reset force	4.0 N
6. self actuating temperature	74 °C
7. maximum current	5.0 A
8. minimum current to actuate	2.0 A
9. actuator electric resistance	0.2 Ω
10. time to actuate at 4 A :	
* time to start	2.5 s
* time to 90% complete	6.0 s
11. time to reset after 10 min on :	
* time to start	3.0 s
* time to 90% complete	7.0 s

Table A-2 - Physical Properties of NITINOL Actuators

PROPERTY		VALUE
I. *Phase Properties*		
1. cooling transformation temp.[1]	(T_T)	52.5 °C
2. heating transformation temp.[1]	(T_T)	66.0 °C
3. latent heat of transformation[2]	(Q_l)	12,620 J/Kg
4. percentage shape memory[3]		4-8%
II. *Physical properties*[3]		
5. density	(ρ)	6.5 gm/cm^3
6. thermal capacitance	(c_p)	883.0 J/kg°C
III. *Mechanical properties*[3]		
7. Young's modulus	(E)	70.0 GPa
8. Yield Strength	(σ_y)	420.0 MPa

1. Reference [16] , 2. Reference [17] and 3. Reference [18]

REFERENCES

1. Baz, A., S.Poh and P.Studer,"Performance of an Active Vibrationn Control System using Piezo-Electric Actuators", J.of Sound and Vibration, Vol.126, No.1, October 1988.

2. Baz, A.,"Experimental Control of Vibrations by Piezo-Electric Bimorphs", Technical report #23185-EG-II, U S Army Research Office , November 1985.

3. Jezequel, L.,"Structural Damping by Slip in Joints", ASME J. of Vibration, Acoustics, Stress and Reliability in Design, Vol.105, No.4, pp.497-504, June 1983.

4. Gaul, L.,"Wave Transmission and Energy Dissipation at Structural and Machine Joints", ASME J. of Vibration, Acoustics, Stress and Reliability in Design, Vol.105, No.4, pp.489-496, 1983.

5. Bailey, T., and J. Hubbard,"Distributed Piezo-Electric Polymer Active Vibration Control of a Cantilever Beam", J. of Guidance, Vol.8, pp. 605-611, Sept.1985.

6. Forward, R.,"Electronic Damping of Orthogonal Bending Modes in a Cylindrical Mast-Experiment", J. of Spacecraft, Vol.18, pp.11-17, 1981.

7. Baz,A.and J.Fedor,"A New Class of Passive Fluid Loop Dampers", Proc. of Symposium DAMPING 89, Wright-Patterson Air Force Base, W.Palm Beach, Florida, 8-10 February 1989.

8. Perkins,J., *Shape Memory Effect in Alloys* , Plenum Press, New York, 1975.

9. Watson, R.," Comparison of the Response of Shape Memory Alloy Actuators Using Air-Cooling and Water-Cooling", Masters Thesis, Naval Postgraduate School, Monterey, California, Dec. 1984.

10. Baz, A., K.Iman and J. McCoy,"Active Control of Flexible Space Structures Using NITINOL Shape Memory Actuator", Technical Report #FQ8671-8700771,Air Force Office of Scientific Research, Oct. 1987.

11. Toda, M., S. Osaka, and E. Johnson,"A New Electro-motional Device", RCA Engineer, Vol. 25, No. 1, pp.24-27, 1979.

12. Aronson, R., (ed.),"Rediscovering Piezo-Electrics", Machine Design, Vol. 56, No.14, pp.73-77, 1984.

13. Nakano, Y., "Hitachi's Robot Hand", Robotics Age, Vol.6, pp.18-20, 1984.

14. Schetky, L.," Shape Memory Effect Alloys for Robotics Devices", Robotics Age, Vol.6, pp.13-17, 1984.

15. Schetky, L.,"Shape- Memory Alloys", Scientific American, pp.74-82, Nov. 1979.

16. Yeager, J.,"A Practical Shape-Memory Electro-Motional Actuator", Mechanical Engineering, Vol. 106, No.7, pp. 52-55, July 1984.

17.Wang, F., Innovative Technology International, Inc., Beltsville, MD , 1986.

18. Benson, R., R.Flot and C.Sandberg, "The Use of Shape Memory Effect Alloys as an Engineering Material", Proc. of 15th National SAMPE Technical Conference, pp.403-414, October 1983.

19. Chajes, A., *Principles of Structural Stability Theory.*, Prentice-Hall, Inc., Englewood Cliffs, NJ , 1974.

20. Paz, M.,*Structural Dynamics : Theory and Computation* ,Von Nostrand Reinhold Co., Second ed., New York, 1985.

N O M E N C L A T U R E

Latin Letters

A	surface area of actuator	m^2
C_a	damping coefficient of actuator	N s/m
c_p	specific heat of actuator material	J/kg^oC
d	diameter of actuator wire	m
d_b	dead band of controller	m
E	Young's modulus of beam	N/m^2
F	phase transformation force	N
F_a	actuator force	N
F_d	damping force of actuator	N s/m
F_{max}	maximum actuator force	N
F_p	applied pneumatic load	N
F_s	spring force of actuator	N
h	heat transfer coefficient	J/m^2s^oC
I	current passing through the actuator	amp
I	area moment of inertia of beam	m^4
J_i	mass moment of inertia of element i	Nms^2/rad
K	stiffness matrix of beam	N/m
L	beam length	m
l	element length	m
m	mass of actuator	kg
m_i	mass of element i	kg
M	mass matrix of beam	kg
n	number of beam elements	
P	total axial force acting on beam	N
Q_l	latent heat of transformation of NITINOL	J/kg
q_i	transverse load (or moment) acting on node i	N, Nm
t	time	s
T_a	ambient temperature	^oC
T_{max}	maximum actuator temperature	^oC
T_T	phase transformation temperature	^oC
X	position along longitudinal axis of beam	m
X_{max}	maximum deflection of actuator	m
Y	transverse deflection of mid-span of beam	m
Y_R	desired transverse position of mid-span of beam	m

Greek Letters

δ_i	linear and angular deflection of beam	m, rad.

ϑ_i	angular deflection of node i	rad.
τ_c	cooling time constant of actuator	s
τ_h	heating time constant of actuator	s
τ_{th}	thermal time constant of actuator	s